

Polyurethane anionomers. II. Phase inversion and its effect on physical properties

Show-An Chen* and Jen-Sung Hsu

Chemical Engineering Department, National Tsing-Hua University, Hsinchu, Taiwan 30043, China

(Received 29 January 1992; revised 15 October 1992)

The two series of polyether polyurethane anionomers discussed in part I, undergo emulsification on addition of water to solutions in methyl ethyl ketone. The phase inversion mechanism depends on the structure of the counterion, ionic content and dispersion temperature. The dispersion process can be divided into three stages: separation of hard segment aggregates due to adsorption of water on their surface, water entering into more disordered and then less disordered hard domains, and finally a rearrangement of agglomerates to form microspheres. Films cast from emulsions have crystallizable soft domains, as do films cast directly from solutions. The dispersion can cause a disruption of the packing arrangement in the hard domains, leading to an increased phase separation for the TEA system and an increased phase mixing for the EDEA system. Films cast from solutions have hard domains dispersed in the continuous phase of soft domains. After dispersion, the hard segments originally distributed in the dispersed phase can be inverted to become a hard domain network or a continuous phase.

(Keywords: poly(tetramethylene oxide); emulsification; dimethylolpropionic acid; counterion; morphology)

INTRODUCTION

Polyurethane (PU) ionomers, in which ionic groups are usually incorporated on the amino groups of the chain extender, have been investigated extensively with regard to their synthesis, morphology and physical properties¹⁻¹¹. By addition of water to an organic solution of the ionomer followed by removal of the organic solvent, a so-called PU emulsion can be obtained. Studies of the mechanism of the emulsification process and of the morphology and physical properties of emulsion-cast films are limited. Dieterich *et al.*¹ proposed the following emulsification mechanism from viscosity measurements. As water is added to an organic solution of PU ionomer, its viscosity first decreases to a minimum owing to a reduction of the ionic association, and then increases owing to a reduced solvation sheath which causes increased alignment of the hydrophobic chain segments; phase separation starts at this stage. Further addition of water produces turbidity, indicating formation of a dispersed phase, and subsequently leads to a drop in viscosity owing to completion of intermolecular and intramolecular aggregation of hydrophobic segments. Finally, the ionic groups are almost all situated on the particle surfaces. Lorenz *et al.*^{12,13} also found a similar variation in solution viscosity during emulsification and reported the tensile strength of emulsion-cast films without, however, comparison with solution-cast films. Chen and Chan¹⁴ studied three series of PU cationomers with various hard segment structures and found that the phase inversion mechanism depends

on the structure of the hard segment, ionic content and dispersion temperature. The dispersion process can be divided into three stages: separation of hard segment aggregates due to adsorption of water on their surface, water entering into disordered and then ordered hard domains, and finally a rearrangement of agglomerates to form microspheres. Films cast from the emulsions have both ordered and disordered hard-segment regions, as do those cast directly from solution. The dispersion can cause a disruption of the order in the hard domains, leading to an increased phase separation for the 4,4'-diphenylmethane diisocyanate (MDI) system and to a slightly increased phase mixing for the hexamethylene diisocyanate (HDI) and toluene diisocyanate (TDI) systems. Solution-cast films have soft domains as the continuous phase in which hard domains are dispersed as a fibrillar network. After dispersion, the hard segments originally distributed in the dispersed phase can be inverted to form a hard domain network or continuous phase.

The preceding paper, part I⁵, discussed the structure/property relations of films cast from methyl ethyl ketone (MEK) solutions of two series of polyether PU anionomers having different counterions. Detailed phase inversion mechanisms during emulsification of the two series of PU anionomer solutions in MEK are proposed on the basis of conductivity and viscosity measurements at the dispersion temperatures of 20 and 60°C. The phase inversion mechanism is affected strongly by the structure of the counterion, ionic content and dispersion temperature. In addition, effects of emulsification at different temperatures on physical properties of the two systems are also investigated. A morphological

*To whom correspondence should be addressed

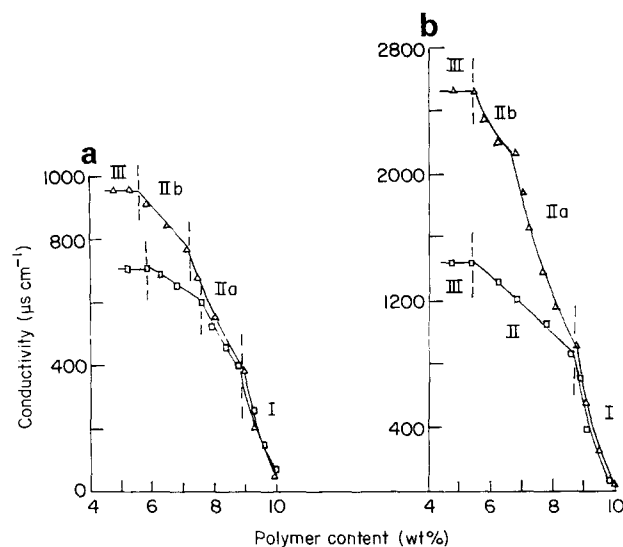


Figure 1 Conductivity of TEA series solutions during addition of water at dispersion temperatures (a) 20°C and (b) 60°C. (□) MT-0.7, (△) MT-1.0

change after dispersion is also elucidated using transmission electron microscopy and property measurements.

EXPERIMENTAL

Descriptions of the chemicals used and procedures for preparation of the two series of PU anionomer solutions in MEK and the instruments and measurement conditions for physical testing of emulsion-cast films are given in part I¹⁵. Emulsification was carried out by adding deionized water slowly with constant agitation at constant temperature (20 and 60°C) to a solution of polyether PU anionomer, 10% by weight, in MEK. During the addition, a conductivity probe and a spindle were used to monitor conductivity and viscosity. When the conductivity of the solution reached a constant level, the phase inversion was considered to be complete and addition of water was stopped. The ionomer solution samples were designated as described in part I. The temperature in the designation is the dispersion temperature.

Conductivity was measured using a conductivity meter from Crison Instrument Co. and viscosity using a Brookfield SynchroLectric viscometer with spindles LVT no. 1-4.

Films for physical testing were prepared by pouring the emulsion into a Teflon mould of inner dimensions 8 cm × 8 cm × 1 cm. After standing at room temperature for 4 days to allow evaporation of the water, the sample was vacuum-dried at 60°C for 48 h to remove any residual moisture. The dry samples so obtained were about 0.3 cm thick and were stored in a desiccator at room temperature before testing.

RESULTS AND DISCUSSION

Phase inversion mechanism during emulsification

In an organic medium, such as MEK or acetone, ionized segments of PU ionomer could be bridged by counterions through coulombic interactions to form a type of 'microionic lattice', as proposed by Dieterich *et al.*¹ on the basis of the observation that the apparent

molecular weight from viscosity measurements increases rapidly with increasing polymer concentration. Thus, it is reasonable to consider that aggregation of hard segments in the films cast from solutions could also occur in the organic solution and affect the phase inversion mechanism. The following observations on conductivity and viscosity variations during the addition of water suggest a mechanism for the phase inversion. Since the mechanism is not supported by direct structural evidence, it should be considered as a hypothesis still in need of testing.

For the two series of solutions of the amine systems, variations in conductivity and viscosity during addition of water at 20 and 60°C are shown in *Figures 1-4*, respectively. The entire emulsification process can be conveniently divided into three stages as indicated on these figures.

In stage I, as water is added slowly to the ionomer solution, it is adsorbed by the carboxylate anions situated on the surface of the hard segment microionic lattices (*Figure 5a*), causing a separation of neighbouring chains and aggregates. Each microionic lattice, which is considered to form in the organic medium, is an aggregation of unsolvated salt segments stabilized by coulombic forces¹. The conductivity of the solution increases and is slightly concave upwards (*Figures 1 and 2*). The viscosity of the solution decreases rapidly to a lower limit (*Figures 3 and 4*). The increase in conductivity and decrease in viscosity indicate that the ionic groups on the surface of the hard-segment microionic lattices are almost completely dissociated. During this stage, the solutions are always clear, indicating that the size of the aggregated hard domains is smaller than the wavelength of visible light (i.e. <0.6 µm).

For the dispersion temperature of 20°C, at the beginning of stage II (stage IIa), as more water is added, it starts to enter the interior of the more disordered hard-segment microionic lattices (*Figure 5b*). The hydrophobic segments (soft segments) lose their solvation sheath, and subsequently aggregate to form aligned hydrophobic aggregates, which eventually

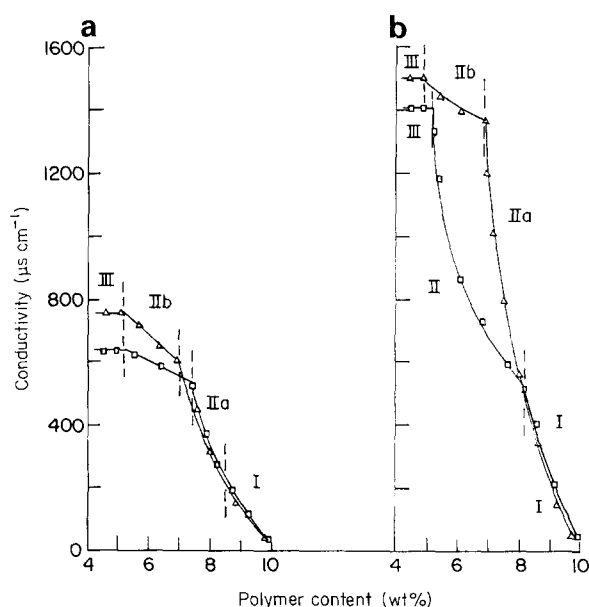


Figure 2 Conductivity of EDEA series solutions during addition of water at dispersion temperatures (a) 20°C and (b) 60°C. (□) ME-0.7, (△) ME-1.0

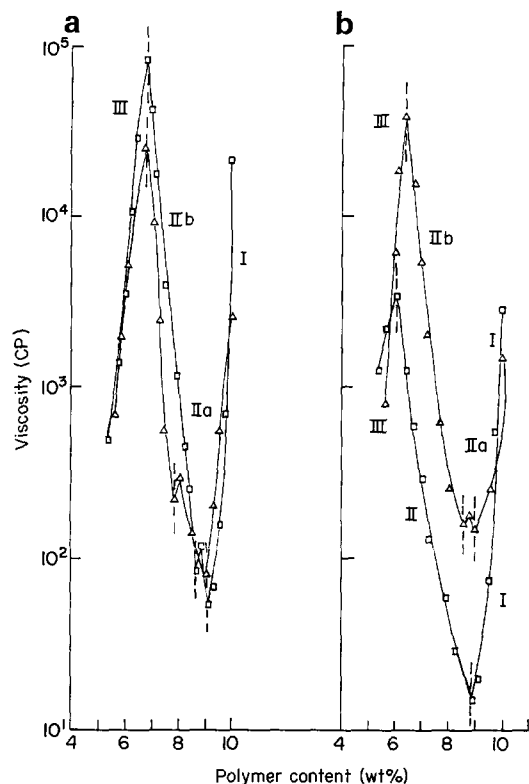


Figure 3 Viscosity of TEA series solutions during addition of water at dispersion temperatures (a) 20°C and (b) 60°C. (□) MT-0.7, (△) MT-1.0

become dispersed phases. The solution becomes turbid and the turbidity increases with further addition of water. During this stage, as water is added, conductivity increases and is slightly concave upwards and slower than in stage I (Figures 1 and 2). This result indicates that water enters less easily into the more disordered hard-segment microionic lattice. The viscosity increases slightly owing to the increased number of hydrophobic aggregates and passes through a small maximum (Figures 3 and 4). The presence of this maximum indicates dissociation of the more disordered hard domains, accompanied by increased association of hydrophobic segments. Further addition of water causes a decrease in viscosity which also supports the idea that some of the more disordered hard-segment microionic lattices are dissociated. At the end of this stage, the two-phase PU ionomer is still continuous, since the less disordered hard-segment microionic lattices are still not dissociated.

In stage IIb, continuing addition of water causes the viscosity to increase sharply to another maximum (Figures 3 and 4), indicating dissociation of the hard-segment less disordered microionic lattices accompanying an increased association of the hydrophobic segments (Figure 5c). The conductivity curves are linear at 20°C and concave upwards at 60°C for an ionic content of 1.0, both with smaller slopes than those in stage IIa (Figures 1 and 2), indicating that the entrance of water into the less disordered hard-segment microionic lattices is more difficult than into the more disordered hard domains in stage IIa. Water enters more easily into the hard-segment less disordered microionic lattices with increasing dispersion temperature and ionic content.

Hydrogen bonds between the urethane groups begin to dissociate at about 40–60°C¹⁶, the dispersion temperature range used. At the dispersion temperature

of 60°C, most of the hydrogen bonds in the less disordered hard domains have been dissociated, allowing more water to enter. This is reflected in the fact that, for an ionic content of 0.7, the conductivity in stage II gives a single curve without distinguishable stages and the viscosity curves exhibit only one maximum. The slopes of the

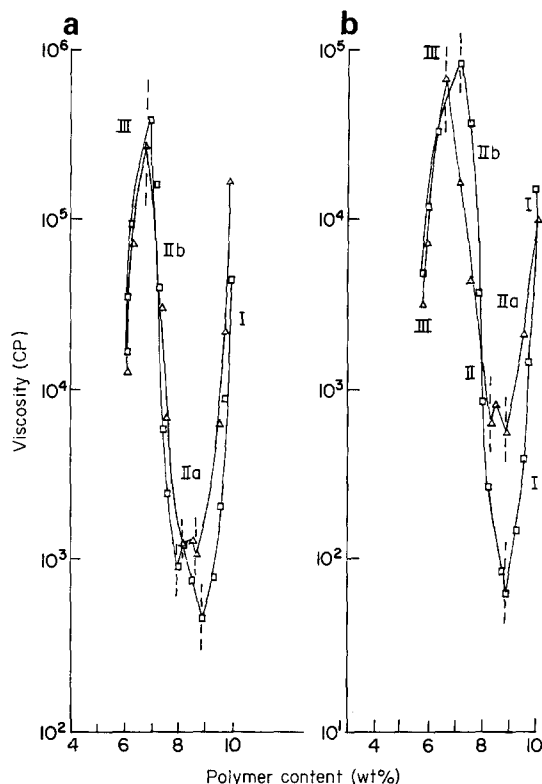


Figure 4 Viscosity of EDEA series solutions during addition of water at dispersion temperatures (a) 20°C and (b) 60°C. (□) ME-0.7, (△) ME-1.0

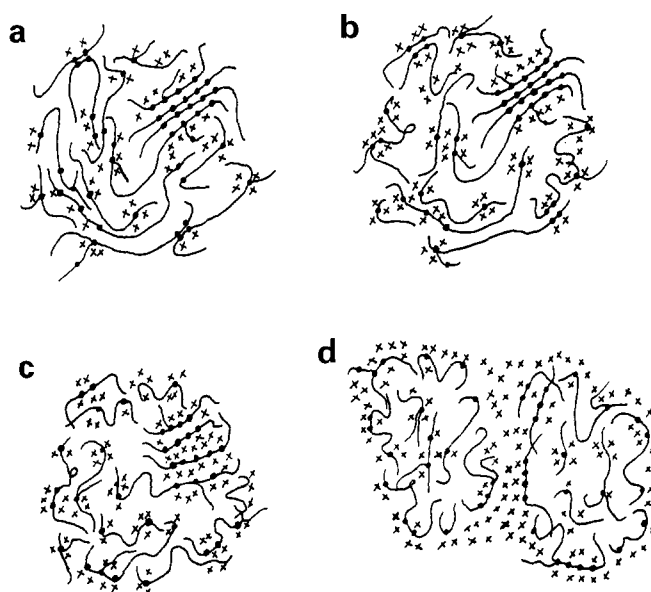


Figure 5 Schematic representation of the emulsification and phase inversion sequence. (—●—●—) Ionized hard segments (with counterions); (—) soft segments; ×, water molecules; solvent molecules are not shown. The aggregates (or hard-segment microionic lattices) composed of aligned hard segments denote less disordered hard domains. Those composed of two unaligned hard segments denote more disordered hard domains. (a) Stage I, (b) stage IIa, (c) stage IIb, (d) stage III

Table 1 Characteristic peaks determined from the dynamic mechanical properties of two systems at dispersion temperatures of 20°C and 60°C

Sample	γ peak (°C)	β peak (°C) (T_{gs})	α peak (°C) (T_{gh})
MT-1.0 ^a	-138	-57	123
MT-1.0-20°C	-139	-59	124
MT-1.0-60°C	-142	-58	123
ME-1.0 ^a	-137	-61	94
ME-1.0-20°C	-139	-56	99
ME-1.0-60°C	-138	-58	96

^a Values of the solution-cast films are taken from part I (ref. 15)

conductivity curves and the conductivities are both at a higher level, indicating that the phase inversion is more complete than at 20°C. A comparison between TEA and EDEA systems at stage IIb shows that the conductivities of the latter are about 0.6 to 0.97 times those of the former. Thus, for the EDEA system, entrance of water into the less disordered hard-segment microionic lattices (Figure 5c) is less extensive than in the TEA system. The results of morphological studies also support this interpretation, as will be discussed later.

In stage III, the viscosity drops sharply and the conductivity remains almost constant. At this stage the phase inversion is complete. The agglomerates have been rearranged to form microspheres. There exists a continuous water-rich liquid phase and a dispersed polymer phase (the polymer particles) swollen with the organic solvent (Figure 5d). Most of the ionic groups of polymer chains subject to phase inversion are situated on the particle surface.

Comparison with PU cationomer

For the PU cationomer PTMO/MDI/MDEA/glycolic acid studied by Chen and Chan¹⁴, the dispersion process has been divided into three stages. In the second stage, the water enters into disordered hard domains (IIa) and ordered hard domains (IIb), respectively. The viscosity-concentration curves have a very significant maximum at stage IIa, and the conductivity-concentration curves have a more significant slope change between stage IIa and stage IIb than those of the present PU anionomers. These differences can be attributed to the different structure of the hard domains. The PU cationomers have a chain extender (MDEA) more symmetrical than the PU anionomers (DMPA), and the former are linear rather than branching as in the latter. These lead to anionomers with no detectable ordering in the hard domains, causing less sharp variations in viscosity and conductivity during the second stage (stage II).

For the above-mentioned two ionomers, the extent of phase inversion increases with increasing ionic content and dispersion temperature.

Structure and properties of films from emulsions

Infra-red (i.r.) spectroscopy. I.r. spectra of the two systems studied here are similar to those of the solution-cast films discussed in part I. The absorption frequencies of the NH and C-O-C groups are the same as in the solution-cast films and show no change with dispersion temperature.

For TEA systems (MT-1.0-20°C and 60°C), the C=O peak shifts upwards by 4 cm⁻¹ and 6 cm⁻¹, respectively.

These results indicate that some of the NH groups previously bonded with C=O groups of urethane now switch to form hydrogen bonds with -COO⁻ groups. Thus disruption of the ordered packing arrangement of the hard domains occurs during the dispersion process.

For the EDEA system after dispersion (ME-1.0-20°C and 60°C), the intensity of the bonded C=O increases as the dispersion temperature increases while that of the free C=O decreases as the dispersion temperature increases. These results indicate that some of the OH groups previously bonded with other OH groups now switch to form hydrogen bonds with C=O groups.

For the two ionization systems, the C=O peaks change upon dispersion; it is clear that the dispersion does change the packing arrangement of the hard segments.

Wide-angle X-ray diffraction (WAXD). Wide-angle X-ray diffraction (WAXD) measurements on the two systems are the same as those of the solution-cast films discussed in part I. Only a single diffuse scattering peak with maximum intensity near 20° (2 θ) was observed, indicating that no crystallinity of either hard or soft segments was detected by WAXD¹⁷.

Dynamic mechanical analysis. Dynamic mechanical measurements on the two systems were carried out, and their transition temperatures, determined from the maxima of the tan δ peaks, are listed in Table 1. For the entire dynamic mechanical curves, only those of the TEA system are shown in Figure 6. Physical interpretation of the three peaks in the tan δ curves is described in part I.

For MT-1.0-20°C (Table 1), the glass transition temperature of the soft domains (T_{gs}) of the emulsion-cast film is 2°C lower than that of the solution-cast film MT-1.0, while the glass transition temperature of the hard domains (T_{gh}) increases by 1°C, indicating that the dispersion leads to a slightly increased phase separation and increased order of hard domains. As the dispersion temperature increases to 60°C, T_{gs} increases by 1°C, while T_{gh} drops by 1°C, indicating that increasing the dispersion temperature leads to a slightly increased phase mixing and decreased order in the hard domains.

For ME-1.0-20°C (Table 1), T_{gs} and T_{gh} of the emulsion-cast film are both 5°C higher than those of the corresponding solution-cast film ME-1.0, indicating that the dispersion leads to an increased phase mixing and

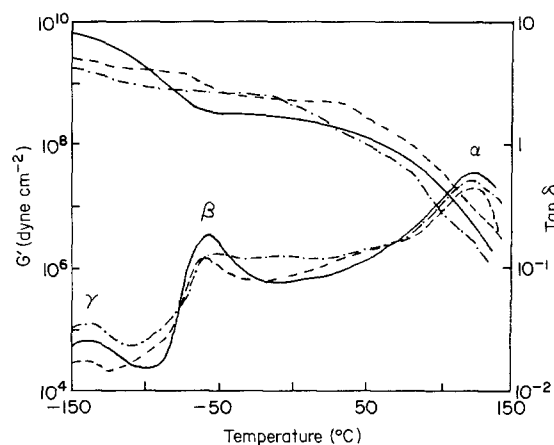
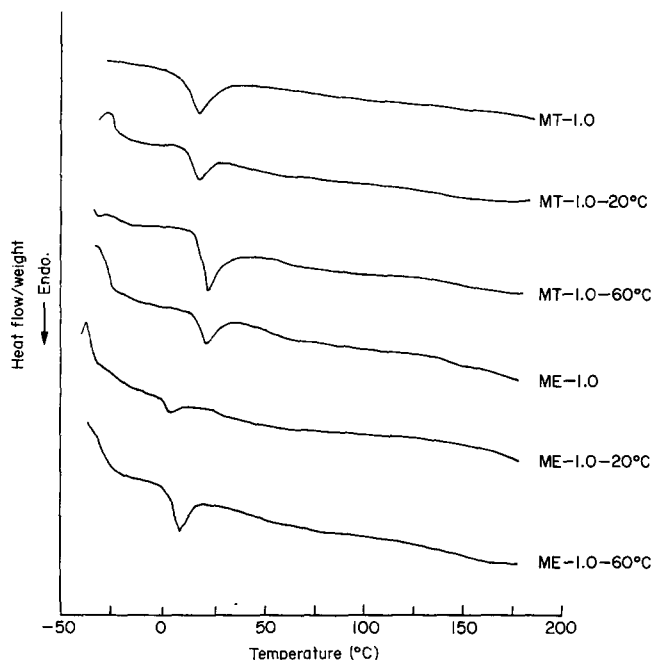


Figure 6 Dynamic mechanical analysis of the MT-1.0 series at dispersion temperatures 20°C (---) and 60°C (-.-). (—) Solution-cast film

Table 2 Characteristic peaks determined from d.s.c. curves for the two systems at dispersion temperatures of 20°C and 60°C

Sample	T_{ms} (°C)	ΔH_{ms} (J g ⁻¹)
MT-1.0 ^a	18.4	4.0
MT-1.0-20°C	16.9	2.8
MT-1.0-60°C	22.0	4.3
ME-1.0 ^a	21.0	3.0
ME-1.0-20°C	2.6	0.9
ME-1.0-60°C	9.1	3.1

^a Values for solution-cast films are taken from part I (ref. 15)

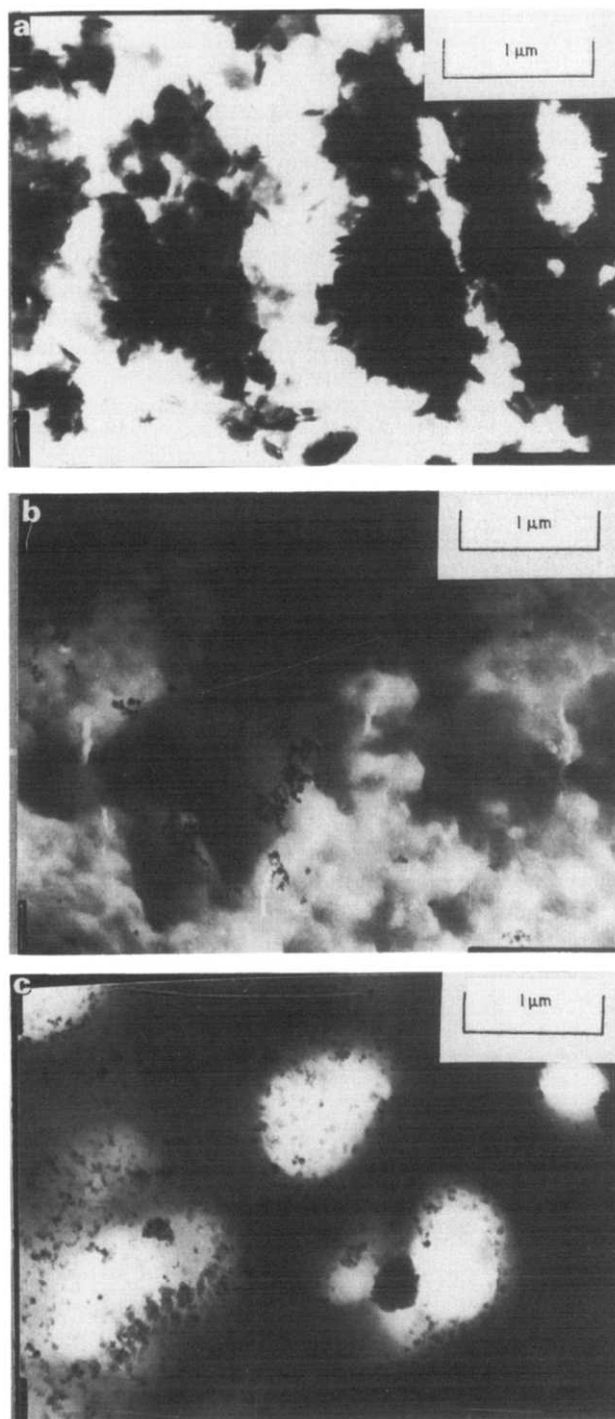
**Figure 7** D.s.c. curves of the films

increased order of the hard domains. As the dispersion temperature increases to 60°C, T_{gs} decreases by 2°C, while T_{gh} drops by 3°C. This result indicates that increasing the dispersion temperature leads to an increased phase separation and decreased order in the hard domains. The results of tensile-elongation measurement also support this interpretation, as will be discussed below.

Differential scanning calorimetry (d.s.c.). D.s.c. curves for the two systems are shown in Figure 7. The temperatures and heats of melting for the characteristic peaks of all samples are listed in Table 2. For all films similar to the solution-cast films, an endothermic peak was found below 25°C (Figure 7), which corresponds to the melting peak of the soft domains^{9,10,17}. There is no evidence to show the presence of ordered hard domains for all systems, as in the solution-cast films.

For the TEA system, the melting temperature (T_{ms}) and heat of melting (ΔH_{ms}) do not change significantly after the dispersion, possibly because the degrees of phase separation are approximately the same before and after dispersion, as indicated by the similar T_{gs} values of the films (Table 1). For the EDEA system after dispersion, T_{ms} is much lower than that of the solution-cast film, possibly due to the smaller crystallite size of the former caused by the lower degree of phase separation as indicated in the d.m.a. result (Table 1).

Morphological changes after dispersion with water. Transmission electron microscopy (TEM) micrographs of the two systems cast from solutions and emulsions are shown in Figures 8 and 9, respectively. The solution-cast film of the TEA system (MT-1.0) shows that hard domains are dispersed in the soft domains (Figure 8a). After dispersion at 20°C, partial phase inversion occurs and some of the hard segments are exposed on the particle surfaces in the emulsion. During film formation, the particles coagulate to form a film with a morphology of interwoven soft and hard domains (Figure 8b). Continuous and dispersed phases are no longer distinguishable. As the dispersion temperature increases to 60°C, more hard segments are inverted. During film formation, the

**Figure 8** TEM micrographs of the TEA system materials: (a) MT-1.0, (b) MT-1.0-20°C, (c) MT-1.0-60°C

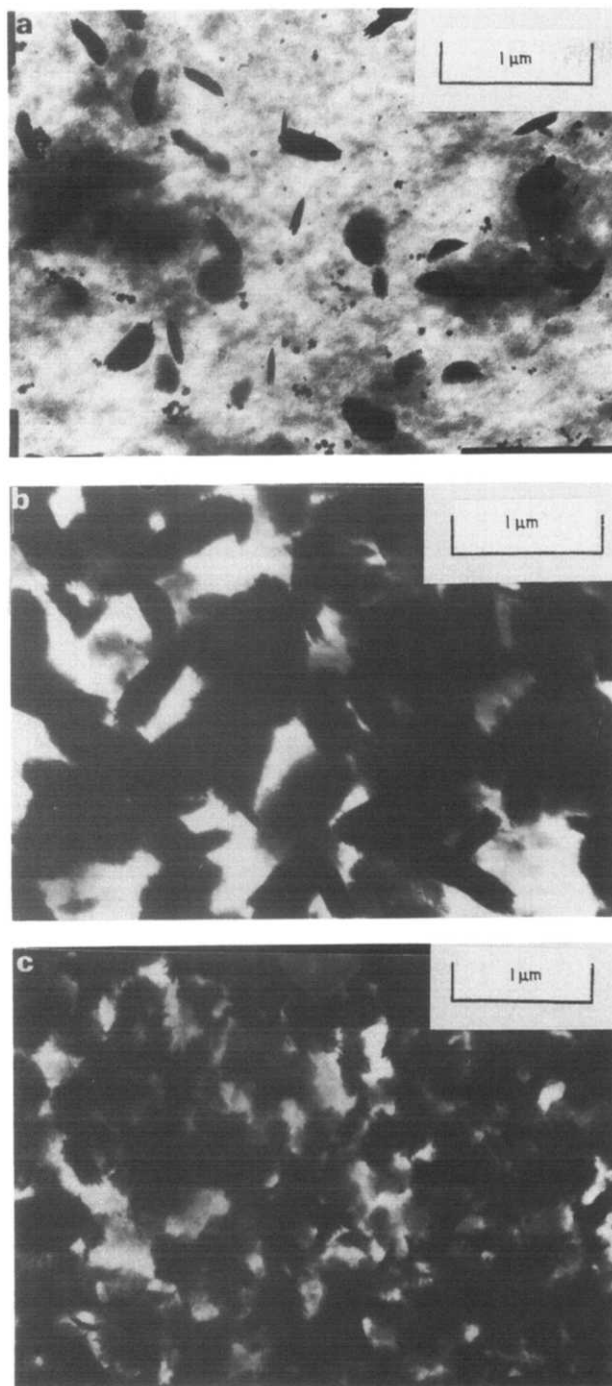


Figure 9 TEM micrographs of the EDEA system materials: (a) MT-1.0, (b) MT-1.0-20°C, (c) MT-1.0-60°C

particles with hard domains on the particle surfaces then agglomerate to form a continuous phase; the soft domains located in the particles then become the dispersed phase (Figure 8c).

For the EDEA system, the solution-cast film (ME-1.0) shows that hard domains are dispersed in the soft domains (Figure 9a). After the dispersion at 20°C, partial phase inversion occurs and some of the hard segments are exposed on the particle surfaces in the emulsion. During film formation, the particles coagulate to form a film with a morphology of interwoven soft and hard domains (Figure 9b). Continuous and dispersed phases are no longer distinguishable. As the dispersion temperature increases to 60°C, more hard segments are inverted, but the phase inversion is not as complete as

that of the TEA system, and the film still has a morphology of interwoven soft and hard domains (Figure 9c). This result is in agreement with the phase inversion mechanism.

Tensile properties. The tensile properties of the two systems are shown in Figure 10. The tensile strength and elongation at break are summarized in Table 3. For the TEA system, with a dispersion temperature of 20°C, the emulsion-cast film has slightly higher tensile strength and lower elongation at break than the solution-cast film. This is due to partial phase inversion to give the interwoven hard/soft domain morphology. The size of hard domains increases resulting from increased order of hard segments as confirmed by the d.m.a. result which leads to higher tensile strength. As the dispersion temperature increases to 60°C, water can penetrate into most parts of the hard domains, causing increased phase inversion but since the TEA counterion is symmetrical, the disruption of the packing arrangement is not significant, leading to tensile properties comparable with those at a dispersion temperature of 20°C.

For the EDEA system, with a dispersion temperature of 20°C, the emulsion-cast films have slightly higher tensile strength and lower elongation at break than the respective solution-cast films. This is due to partial phase inversion to give the interwoven hard/soft domain morphology. The size of hard domains increases resulting from increased order of the hard segments as confirmed by d.m.a., leading to higher tensile strength. As the dispersion temperature increases to 60°C, more water enters the hard domains and changes the packing

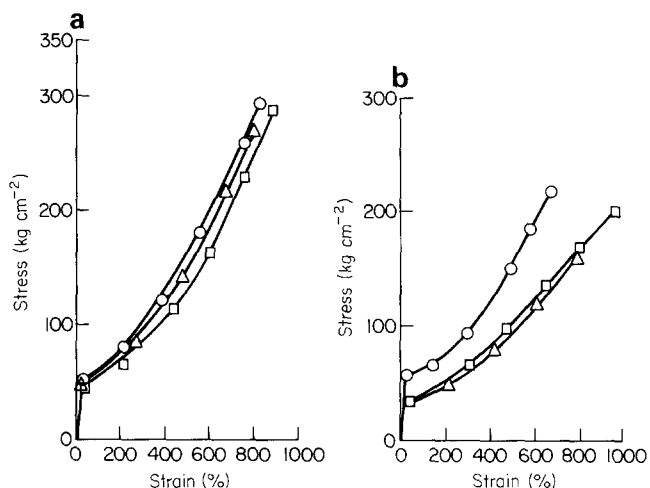


Figure 10 Stress-strain curves of (a) MT-1.0 and (b) ME-1.0 series at dispersion temperatures (O) 20°C and (Δ) 60°C. (□) Solution-cast film

Table 3 Characteristic values for tensile-elongation curves of the two systems at dispersion temperatures of 20°C and 60°C

Sample	Tensile strength (kg cm ⁻²)	Elongation (%)
MT-1.0 ^a	190	892
MT-1.0-20°C	296	816
MT-1.0-60°C	281	809
ME-1.0 ^a	200	976
ME-1.0-20°C	218	680
ME-1.0-60°C	163	795

^a Values for solution-cast films are taken from part I (ref. 15)

arrangement of hard domains, but they are still in partial inversion. The hard domains become more randomly distributed, as shown in the morphological studies, which causes the hard segment order to decrease, leading to decrease in tensile strength.

Comparison with PU cationomer. For the PU cationomer PTMO/MDI/MDEA/glycolic acid studied by Chen and Chan¹⁴, the emulsion-cast films have detectable order in their hard domains, but for the PU anionomers there is no detectable hard-segment ordering in the hard domains and only soft segment crystallites exist in the soft domains. This must be because the chain extender of the anionomers (DMPA) is more asymmetrical than that of the cationomers (MDEA) and the resulting anionomers are branching instead of linear like the cationomers. For both cationomers and anionomers, the dispersion process can cause a disruption of the packing arrangements in the hard domains, leading to increased phase separation or phase mixing between the soft and hard domains.

Let us compare the morphology of cationomer PTMO/MDI/MDEA/glycolic acid¹⁴ with the present anionomer. The unionized film of the former shows a morphology with soft domains as the continuous phase and hard domains as a fibrillar network in the continuous phase. For the anionomer, the unionized film shows a morphology with soft domains as the continuous phase and hard domains as the dispersed phase. After dispersion at 20°C, both cationomers and anionomers show a morphology of interwoven soft and hard domains. Continuous and dispersed phases are no longer distinguishable. As the dispersion temperature increases to 60°C, more hard segments are inverted. For both the cationomer and the TEA system of the anionomer, the morphology shows the soft domains dispersed in the continuous phase of hard domains. For the EDEA system of anionomer, the phase inversion is not as complete as in the cationomer and TEA system of the anionomer, and the film still has a morphology of interwoven soft and hard domains.

CONCLUSIONS

The mechanism of phase inversion can be divided into three stages. In stage I, the water is adsorbed by ionic groups situated on the surface of the hard-segment microionic lattices. In stage II, the water enters the more disordered hard domains first and then the less disordered hard domains for two systems. For the TEA system, however, the water enters into the hard domains more

completely than for the EDEA system. In stage III, the phase inversion is complete. The extent of phase inversion is affected by the structure of the counterion, ionic content and dispersion temperature.

Films cast from emulsions have crystallizable soft-segment regions, as do films cast directly from solutions. The dispersion can cause a disruption of the packing arrangements of the hard domains, leading to increased phase separation for the TEA system and an increased phase mixing for the EDEA system.

Solution-cast films have a morphology with hard domains dispersed in the soft domains. After dispersion, the hard segment originally distributed in the dispersed phase can be inverted to form a hard-domain network or continuous phase.

ACKNOWLEDGEMENTS

The authors wish to thank the National Science Council of the Republic of China for financial aid through the project Studies on Emulsion Polymer Systems, NSC 79-0405-E007-05.

REFERENCES

- 1 Dieterich, D., Keberle, K. and Witt, H. *Angew. Chem. Int. Edn* 1970, **9**, 40
- 2 Hwang, K. K. S., Yang, C. Z. and Cooper, S. L. *Polym. Eng. Sci.* 1981, **21**, 1027
- 3 Yang, C. Z., Hwang, K. K. S. and Cooper, S. L. *Macromol. Chem.* 1983, **184**, 651
- 4 Speckhard, T. A., Hwang, K. K. S., Yang, C. Z., Laupan, W. R. and Cooper, S. L. *J. Macromol. Sci.-Phys.* 1984, **B23**, 175
- 5 Yu, X.-H., Nagarajan, M. R., Grasel, T. G., Gibson, P. E. and Cooper, S. L. *J. Polym. Sci., Polym. Phys. Edn* 1985, **23**, 2319
- 6 Yu, X., Nagarajan, M. R., Li, C., Gibson, P. E. and Cooper, S. L. *J. Polym. Sci., Polym. Phys. Edn* 1986, **24**, 2681
- 7 Chen, S. A. and Chan, W. C. *J. Polym. Sci., Polym. Phys. Edn* 1990, **28**, 1499
- 8 Al-Salah, H. A., Frisch, K. C., Xiao, H. X. and Mclean, J. A. Jr *J. Polym. Sci., Polym. Chem. Edn* 1987, **25**, 2127
- 9 Lee, D. C., Register, R. A., Yang, C. Z. and Cooper, S. L. *Macromolecules* 1988, **21**, 1005
- 10 Miller, J. A., Hwang, K. K. S. and Cooper, S. L. *J. Macromol. Sci.-Phys.* 1983, **B22**, 321
- 11 Al-Salah, H. A., Mclean, J. A. Jr, Frisch, K. C. and Xiao, H. X. *J. Macromol. Sci.-Phys.* 1987, **B26**, 447
- 12 Lorenz, O., Haulena, F. and Klebon, O. *Angew. Makromol. Chem.* 1973, **33**, 159
- 13 Lorenz, O. and Hick, H. *Angew. Makromol. Chem.* 1978, **72**, 115
- 14 Chen, S. A. and Chan, W. C. *J. Polym. Sci., Polym. Phys. Edn* 1990, **28**, 1515
- 15 Chen, S.-A. and Hsu, J.-S. *Polymer* 1993, **34**, 2769
- 16 Sung, C. S. P. and Schneider, N. S. *Macromolecules* 1977, **10**, 452
- 17 Kazmierczak, M. E., Froncs, R. E., Buchanan, D. R. and Gilbert, R. D. *J. Polym. Sci., Polym. Phys. Edn* 1989, **27**, 2173